Research Article

Journal of MASS SPECTROMETRY

Received: 17 November 2010 Accepted: 18 February 2011 Published online in Wiley Online Library: 2011

(wileyonlinelibrary.com) DOI 10.1002/jms.1906

Application of complementary mass spectrometric techniques to the identification of ketoprofen phototransformation products

Tina Kosjek,* Silva Perko, Ester Heath, Bogdan Kralj and Dušan Žigon

Ketoprofen (KP) is a nonsteroidal anti-inflammatory drug, which during UV irradiation rapidly transforms into benzophenone derivatives. Such transformation products may occur after topical application of KP, which is then exposed to sunlight resulting in a photo-allergic reaction. These reactions are mediated by the benzophenone moiety independently of the amount of allergen. The same reactions will also occur during wastewater or drinking water treatment albeit their effect in the aqueous environment is yet to be ascertained. In addition, only a few such transformation products have been recognised. To enable the detection and structural elucidation of the widest range of KP transformation products, this study applies complementary chromatographic and mass spectrometric techniques including gas chromatography coupled to single quadrupole or ion trap mass spectrometry and liquid chromatography hyphenated with quadrupole–time-of-flight mass spectrometry. Based on structural information gained in tandem and multiple MS experiments, and on highly accurate molecular mass measurements, chemical structures of 22 transformation products are proposed and used to construct an overall breakdown pathway. Among the identified transformation products all but two compounds retained the benzophenone moiety – a result, which raises important issues concerning the possible toxic synergistic effects of KP and its transformation products. These findings trigger further research into water treatment technologies that would limit their entrance into environmental or drinking waters.

Keywords: ketoprofen; transformation product; mass spectrometry; identification; photodegradation

INTRODUCTION

Ketoprofen [2-(3-benzoylphenyl)propanoic acid] (KP) is a common nonsteroidal anti-inflammatory drug important for its analgesic, antipyretic and anti-inflammatory activity. Despite its success, it is associated with certain adverse effects, such as peptic ulcer, acute renal failure, bronchospasm[1] and skin photosensitivity disorders including phototoxic, after oral absorption, and photo-allergic after topical application.[2–4] Whereas phototoxicity is unrelated to the immunity response, i.e. every person administered the drug could be affected if exposed to sunlight (UV radiation), the photo-allergic reaction is a hypersensitivity disorder of the immune system and symptom severity is neither related to dosage nor the intensity of the UV radiation.[3,4] Therefore, the photo-allergic reactions may arise not only from the topical KP formulations but also from potable and environmental waters, where KP is commonly found.[5,6] It is considered that both pharmacological mechanisms correlate to each other in that the generation of free radicals from the photolabile KP molecule attack human cells (phototoxicity) and bind to neighbouring skin proteins so that the antigen is grown (photo-allergy).[7] These photosensitivity reactions are associated with the benzophenone chromophore incorporated into the KP structure.[8,9] Besides the parent compound, there are also the radical intermediates[10] and the final phototransformation products (TPs) formed by the rapid KP decomposition under UV irradiation that preserve the benzophenone chromophore and are responsible for the photosensitisation observed *in vivo*, via the formation of oxidative stress.[4] These compounds include 3-ethylbenzophenone (EtBP),[10] 3-acetylbenzophenone (AcBP),[10,11] 3-(α-hydroxyethyl)-benzophenone[10] and α-(3-ethylphenyl)phenylmethanol.[10] The presence of several dimeric photoproducts has also been suggested.[10–12] To date, research has focused on the *in vivo*[9] and *in vitro*[8,9,13] phototoxicity of KP and its benzophenone TPs, and the photochemical mechanisms of their degradation routes.[11,12,14] Further breakdown of the benzophenone ring system including its cleavage would presumably minimise the skin photosensitisation reactions mediated by the benzophenone ring system, which to our knowledge is yet to be reported.

Mass spectrometry is considered a principal tool for identifying TPs, especially since it enables an efficient analysis of trace amounts of analytes in complex organic mixtures. Such complicated environmental or biological samples require separation of components prior to mass spectrometric analysis, which justifies the use of hyphenated techniques such as GC-MS or LC-MS. In this work, we applied three mass spectrometers, a single-stage quadrupole (Q) and an ion trap (IT) both hyphenated to a GC, and a quadrupole–time-of-flight (QqToF) MS coupled to an LC. In the Q mass analyser, the ions generated in the source undergo electron impact (EI) fragmentation, which results in complex, ambiguous spectral data and hence in nonselectivity that is its main disadvantage.[15] In contrast, the IT mass detector has the unique ability to isolate and to accumulate ions. By iterating ion trapping

* *Correspondence to: Tina Kosjek, Department of Environmental Sciences, Jožef Stefan Institute, Jamova 39, 1000 Ljubljana, Slovenia. E-mail: tina.kosjek@ijs.si*

Department of Environmental Sciences, Jožef Stefan Institute, Ljubljana, Slovenia

and scanning – it allows the generation of collision-induced dissociation (CID) spectra of the parent and fragment ions (and their fragment ions), thus increasing the level of confidence in assigning a particular structure.[15] Alternatively, the hybrid QqToF, in which the final resolving mass filter of a triple Q is replaced by a ToF analyser, not only allows MS^2 operation but also has the necessary accuracy and resolution to give exact-mass measurements. Together with MS methods, both chromatographic techniques complement each other to account for a wide range of polarity, acido-basic characteristics and different functional groups, which fits our goal of determining the highest possible number of TPs formed during UV degradation of KP. Accordingly, the main objective of this work is to demonstrate an application of complementary chromatographic and mass spectrometric techniques for identification of the TPs formed during the UV breakdown of KP and to integrate them into a breakdown pathway.

EXPERIMENTAL

Standards, reagents and chemicals

KP (3-benzoyl-α-methylbenzeneacetic acid, CAS: 22 071-15-4) was of $\geq$98% purity and was obtained from Sigma (St. Louis, MO, USA). 3-AcBP (CAS: 66 067-44-5) was purchased at Synchem OHG (Felsberg-Altenburg, Germany). 3-Isopropyl-benzophenone (iPrBP) and 3-ethylbenzophenone (EtBP) were synthesised using Friedel-Crafts alkylation at Faculty of Chemistry and Chemical Engineering, University of Ljubljana (Ljubljana, Slovenia). Two internal standards, ibuprofen and ibuprofen-d3, were applied. Ibuprofen [2-(4-(2-methylpropyl)phenyl)propanoic acid, CAS: 15 687-27-1] was of 98% purity and was obtained from Sigma (St. Louis, MO, USA), while ibuprofen-d3 (α-methyl-d3) was purchased from Dr Ehrenstorfer GmbH (Ausburg, Germany). The derivatising agents were *N*-methyl-*N*-[*tert*-butyldimethylsilyl]trifluoroacetimide (MTBSTFA), which was purchased at Acros Organics (NJ, USA), and *N*-methyl-*N*-[trimethylsilyl]trifluoroacetamide (MSTFA), obtained from Sigma Aldrich (St. Louis, MO). All applied solvents (ethylacetate, acetone, acetonitrile, methanol, MilliQ) and chemicals (hydrochloric acid 37%, formic acid 50% and hydrogen peroxide 30%) were of analytical grade purity.

UV irradiation

One-litre tap water solutions of individual test compounds (KP, EtBP and AcBP) with an initial concentration of 0.6 µM were exposed to UV irradiation. Its duration depended on an elimination efficiency of each test compound, involving three time intervals: 0–20, 0–90 and 0–435 min. Treatment was carried out using a low pressure (LP) monochromatic UV lamp with a peak emission at 254 nm and a medium pressure (MP) lamp with pyrex glass filter. Due to high resistance of EtBP and AcBP to UV irradiation, the efficiency of photocatalysis was tested by adding 0.01% (v/v) H_2O_2 into the test solutions prior to 9-min irradiation by LP lamp.

Sample preparation

Sample preparation was based on solid phase extraction (SPE) using an Oasis™ Hydrophilic-Lipophilic Balance (HLB) reversed-phase sorbent (Waters, Corp., Milford, MA, USA). The extraction was performed on parallel samples in acidic and neutral conditions. One series of 200-ml samples was acidified to pH 2–3 with 37% HCl, while in the second series, the matrix pH was left unadjusted (pH 6). The SPE cartridges were first conditioned with 3 ml of ethylacetate and 3 ml of methanol, equilibrated with 3 ml of MilliQ water (pH 2–3 water in case of acidified sample matrix) and enriched at a flow-rate of approx. 2 ml min^{-1}. The cartridges were then dried for 30 min under vacuum and eluted with 1 ml of acetone, 1 ml of ethylacetate/acetone (7 : 3) and 1 ml of ethylacetate. The combined eluant was evaporated to dryness with nitrogen. The extracts were then dissolved in either 0.5 ml of ethylacetate for analysis by gas GC-MS or in 0.5 ml of 1 : 4 acetonitrile/water for LC-MS analysis. For derivatisation, 30-µl MTBSTFA or MSTFA was added to the ethylacetate extracts and left to react at 60 °C for 1 h. Two internal standards were spiked into the water samples prior to the SPE, where ibuprofen-d3 (2.4 nM) was used for quantification of low-level compounds, and ibuprofen (0.58 µM), which was used for quantification of high-level compounds.

Instrumental analysis

GC-MS

HP 6890 series (Hewlett-Packard, Waldbron, Germany) gas chromatograph fitted with a single quadrupole mass selective detector (GC-MSD) was used. The GC oven was programmed as follows: an initial temperature of 65 °C was held for 2 min, then ramped at 30 °C/min to 180 °C, at 7 °C/min to 280 °C, at 40 °C/min to 300 °C, and finally held for 3 min. The total GC run time was 22.44 min. A DB-5 MS 30 m × 0.25 mm × 0.25 µm (Agilent J&W, CA, USA) capillary column was used, with He as the carrier gas (37 cm s^{-1}). One-microlitre samples were injected at 250 °C in splitless mode, and the transfer line was maintained at 280 °C. The MS was operated in EI ionisation mode at 70 eV. In SCAN mode, masses from *m/z* 50 to 550 were scanned, while in SIM mode, target fragment ions were modified depending on the target compounds. Where possible, one quantification ion (normally the base peak fragment ion) and two confirmation ions per compound were followed. The GC-MSD used Chemstation software for instrumental control and data processing.

GC-MS/MS

A Varian 450-GC hyphenated with an ion trap 240-MS mass spectrometer (GC-IT) was employed for MS/MS analyses. For chromatographic separation a Varian, Inc. FactorFour™ VF-5 ms (30 m × 0.25 mm × 0.25 µm) analytical column was used, and the instrument was operated under the same chromatographic conditions (GC oven, gas flow, injector and interface temperatures) as GC-MSD. One-microlitre samples were injected in splitless mode, kept until 0.5 min, and then split 1 : 50. The IT was operated in EI ionisation mode with an external ionisation source, where in the full scan type masses from 70 to 400 *m/z* were scanned using an automatic gain control prescan to achieve target TIC of 20 000 counts. For further mass fragmentation in the IT cavity, the MS/MS and MS^n ion preparation modes in the resonant waveform were utilised. MS Workstation v6.9.3 software was used for control, automation and processing.

LC-MS/MS

The chromatographic separation was performed on a Waters Acquity ultra-performance liquid chromatograph (Waters Corp., Milford, MA, USA), equipped with a binary solvent delivery system and an autosampler. The injection volume was 5 µl. Separation was achieved using a 3-cm-long Acquity UPLC™ BEH C_{18} (Waters

Journal of MASS SPECTROMETRY

Corp., Milford, MA, USA) column with 1.7-μm particle size and 2.1-mm internal diameter. Compounds were analysed under positive [ESI(+)] and negative [ESI(−)] ion conditions. In ESI(+) the mobile phases (A) MilliQ water and (B) acetonitrile were used, while in ESI(−) water was replaced by 0.1% formic acid as the mobile phase A, whereas other LC conditions were kept unchanged. The elution gradient was linearly increased from 20 to 80% B in 6 min, decreased back to 20% in 1 min and then finally kept isocratic for 1 min. The total runtime was 8 min. Flow rate was 0.2 ml min^{-1} and the column temperature was maintained at 40 °C. The UPLC system was interfaced to a hybrid quadrupole orthogonal acceleration time-of-flight mass spectrometer (QqToF Premier, Waters, Milford, MA, USA). The instrument was equipped with an electrospray ionisation interface operating in ESI(−) and ESI(+). The capillary voltage was set to 2.8 and 3.0 kV in ESI(−) and ESI(+), respectively, while the sampling cone voltage was varied between 30 and 40 V. Source and desolvation temperatures were set to 120 and 200 °C, respectively. The nitrogen desolvation gas flow rate was 530 l h^{-1}. For MS experiments, the first quadrupole was operated in *rf*-only mode, while detection was performed in the ToF mass analyser. MS data were acquired over an *m/z* range 100–1000 at collision energy of 4 V. For MS/MS operation, the acquisition range was between *m/z* 50 and 1000, and argon was used as the collision gas at a pressure of 4.5×10^{-3} mbar in the T-wave collision cell. The MS/MS experiments were performed with collision energy, varied between 10 and 40 V, to generate product ion spectra providing the most structural information. Data were collected in centroid mode, with a scan accumulation time set to 0.25 s and an interscan delay of 0.02 s. The data station operating software was MassLynx v4.1. Prior to analysis, the instrument was calibrated over a mass range 50–1000, using a sodium formate calibration solution. Reproducible and accurate mass measurements, at a mass resolution of 10 000, were obtained using an electrospray dual sprayer with leucine enkephalin ($[M - H]^- = 554.2615$, $[M + H]^+ = 556.2271$) as the reference compound. The latter was introduced into the mass spectrometer alternating with the sample via Waters Lock Spray device. Elemental composition of TPs was calculated from accurate masses determined by HRMS at following conditions: C:0–80, H:0–120, N:0–8, O:0–30; ±5.0 ppm tolerance; Double bond equivalent (DBE): min = −1.5, max = 50.0.

Detection approaches, identification and quantification

To include broadest range of TPs, screening was made by operating the GC-MS/(MS) and LC-MS/MS analyses on parallel samples. The detection of TPs in the GC samples was made either by comparing the total or extracted ion chromatograms of the treated samples with those of the control. In the LC-MS/MS analysis, data were acquired in centroid mode and afterwards processed by the MetaboLynx™ application manager embedded into MassLynx v4.1. software (Waters). The algorithm was programmed to detect products of expected transformation pathways (i.e. hydroxylation, decarboxylation and hydroxylation + desaturation) and also to detect unexpected components. The latter were examined in *m/z* 150–300 scanning range with 10 Da size of a step scan. Metabolite traces were searched in the time window 0.50–5.00 min at 0.05-min peak separation. The presence of transformation products was investigated in treated samples, while untreated samples were used as control samples.

Depending on the capabilities of the MS instrumentation, we employed two established strategies to determine the identity of unknown compounds, based on (a) structural information gained in MS, tandem (MS^2) or multiple (MS^n) MS experiments and (b) highly accurate molecular mass measurements.

Quantitative analysis was performed on GC-IT by automatic data processing using MS Workstation software. The calibration curves were prepared in the relevant concentration range from 5 to 600 nM by spiking the reference standards of KP, EtBP and AcBP into tap water. Six calibration points were prepared following the SPE procedure as described in the Section on Sample preparation. Both derivatisation agents and both internal standards were taken into account. The coefficients of determination (R^2) ranged from 0.9926 to 0.9999.

RESULTS AND DISCUSSION

The following two sections describe mass-spectrometric identification of TPs formed by UV breakdown of KP. The results of GC-MS identification involve the fragment ions obtained by Q and IT mass analysers and are summarised in Fig. 1 and Table 1. Table 2 includes the LC-MS data on KP and TPs, while their chemical structures are illustrated in Fig. 2.

Identification of TPs by GC-MS

The three most notable TPs observed in the GC chromatograms of UV-treated KP samples eluted at 10.86 min (TP-1), 12.68 min (TP-2) and 13.18 min (TP-3). As evident in Table 1, the molecular weight (MW) of KP is 254, whereas MW of TP-1 shows a 44 Da decrease from the parent compound suggesting its decarboxylation. The MW of TP-3 is 16 Da higher than that of TP-1, which is indicative of a hydroxylated intermediate, and TP-2 yields 2 Da lower MW than TP-3, thus suggesting its oxidised form. Figure 1 shows how the structures of TP-1, TP-2 and TP-3 and the parent compound (KP) yield a phenyl fragment ion with *m/z* 77 and a *m*-substituted benzoyl residual at *m/z* 177, 133, 147 and 149 for KP, TP-1, TP-2 and TP-3, respectively. Furthermore, all four compounds show an abundant benzoyl fragment ion at *m/z* 105, whereas *m/z* 181 implies a benzophenone ring system in case of KP, TP-1 and TP-2. TP-3 is an exception, where the 2 Da higher fragment ion at *m/z* 183 suggests a hydrogenated diphenylmethanol ring system. The remaining fragment ions indicate decarboxylation at *m/z* 209 in case of KP and cleavage of a methyl group at *m/z* 209 and 211 for TP-2 and TP-3, respectively. Based on the EI mass fragmentation, the TPs discussed herein were tentatively identified as EtBP (TP-1), AcBP (TP-2) and *m*-acetyl-1,1-diphenylmethanol (TP-3).

TP-4 eluted at 9.83 min and it was formed in the long-term LP irradiation of EtBP samples in TW matrix in highest amounts but was also present in the MQ using both the LP and MP lamp. As described in Table 1 and illustrated in Fig. 1, the compound with a molecular mass 196 revealed fragment ions at *m/z* 181 indicating the cleavage of a methyl group from a characteristic benzophenone fragment ion. The EI mass spectrum also shows the 3-methylbenzoyl fragment ion at *m/z* 119 and benzoyl at *m/z* 105. The fragmentation of 3-methylbenzophenone (TP-4) was confirmed by EI-MS/MS experiments and a positive match (91%) in the National Institute of Standards and Technology (NIST) library.

Derivatisation with silylating agents MTBSTFA and MSTFA was performed on pre-analysed GC-MS samples to enhance the chromatographic response of less volatile TPs and to facilitate their structural elucidation, e.g. by indicating the presence of a carboxyl or hydroxyl moiety in a TP structure. MTBSTFA yields *tert*-butyldimethylsilyl (MTBS) esters or ethers, and is the most

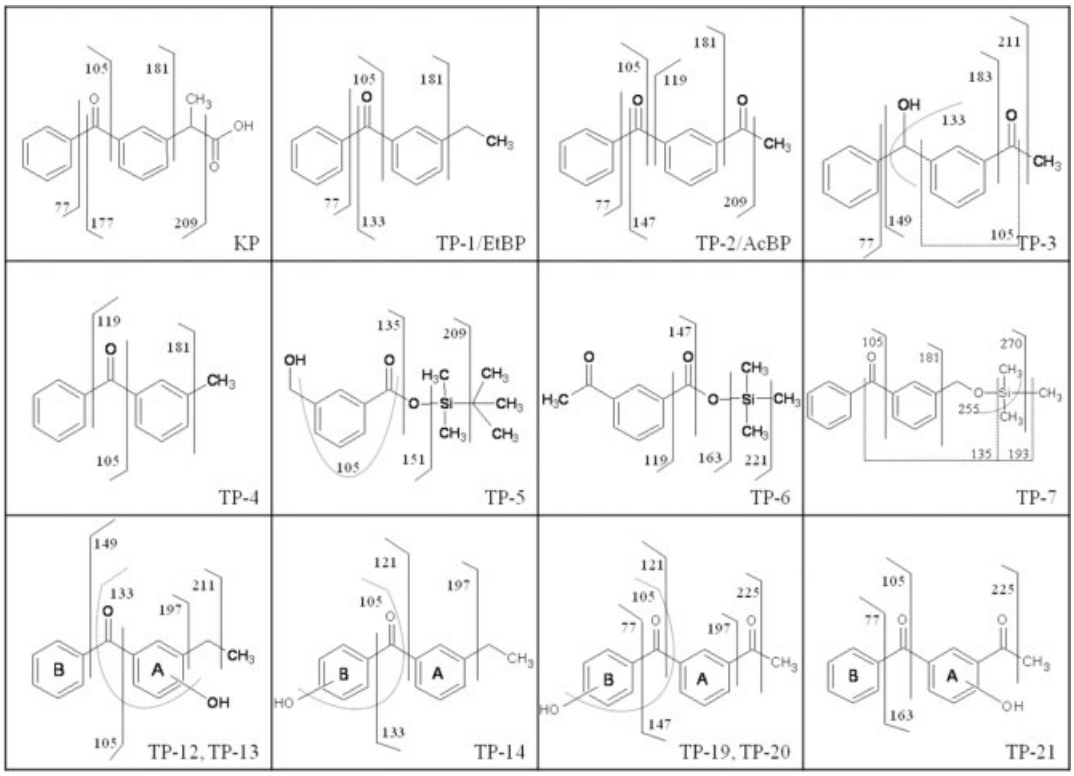

Figure 1. KP and TPs: illustration of fragment ions obtained by EI.

commonly applied silylating agent,[16] probably due to the greater thermal and hydrolytic stability of the derivatives. EI-MS spectra of the MTBS derivatives show a characteristic MS fragmentation, which together with a higher molecular mass of a derivative improves the reliability and detectability of the analyses.[17] A major drawback is its lower reactivity compared with the trimethylsilyl (TMS) derivatives producing reagents,[18] such as MSTFA. The derivatisation enabled us to detect TP-5, TP-6 and TP-7 eluted from the GC column at 9.88, 8.49 and 12.02 min, respectively. TP-5 is an unstable intermediate which is quickly degraded under intense irradiation. It was detected and identified in samples obtained from short-term MP irradiation of EtBP, and trace levels were also formed in EtBP/LP and KP/MP samples. The compound was extracted only under acidic sample preparation conditions. TP-5 was detected as a MTBS ester with a molecular ion at *m/z* 266 and a cleavage of *tert*-butyl group $[M - 57]^+$ at *m/z* 209, a typical fragmentation pattern for MTBS derivatives.[16] The remaining fragment ions are indicative of the cleavage of a *tert*-butyl-dimethylsilyl group to form the deprotonated molecular ion of the underivatised molecule at *m/z* 151, the cleavage of an oxygen to form *m/z* 135 and a characteristic benzoyl fragment ion at *m/z* 105 (Fig. 1). Furthermore, the EI-MS^n experiments yielded *m/z* 121, which is indicative for phenyl-carboxyl fragment ion, suggesting that the structure of TP-5 corresponds to 3-(hydroxymethyl)benzoic acid.

TP-6 was detected as a TMS derivative with a base fragment ion at *m/z* 211, resulting from the cleavage of a methyl group from TMS ending. The deprotonated molecular ion of the underivatised compound is found at *m/z* 163, which further fragments to *m/z* 147 and 119 by cleaving an oxygen or CO_2 group, respectively. The fragment ion *m/z* 119 is indicative for acetylphenyl fragment ion as already shown for TP-2 fragmentation (Fig. 1). It is therefore assumed that TP-6 is an *m*-acetyl-benzoic acid. Another TMS derivative detected by GC-MS was TP-7, yielding the following fragment ions: the benzoyl at *m/z* 105, benzophenone at *m/z* 181 and 135 indicating an underivatised TP-7 after a phenyl ring is cleaved. The remaining three fragment ions in the chemical structure were *m/z* 270 formed by cleavage of a methyl group from a TMS derivative, and *m/z* 193 and 255 formed with subsequent cleavages of a phenyl and a methyl group.

During photocatalytic degradation of EtBP with the addition of 0.01% H_2O_2 several new TPs emerged in GC chromatograms, among them TP-12, TP-13 and TP-14 were most notable. Table 1 shows their retention times and describes their mass spectra. All three compounds have a MW 226, which is 16 Da higher than EtBP from which the compounds were formed. Their mass spectra show cleavage of a methyl group at *m/z* 211, while *m/z* 197 replaces 181 in case of KP, TP-1, TP-2 and TP-4, indicating a hydroxylated benzophenone ring system. Furthermore, TP-12, TP-13 and TP-14 involve a phenyl (*m/z* 77) and benzoyl (*m/z* 105) fragment ions, as well as *m/z* 133, which analogously to TP-1 indicates an *m*-ethyl-benzoyl fragment. The crucial fragment ion in the mass spectra of TP-12 and TP-13 is *m/z* 149 (Table 1, underlined), which shows a 16 Da increase from *m/z* 133, suggesting that hydroxylation occurred on the phenyl ring marked A (Fig. 1). The compounds TP-12 and TP-13 show identical fragment ions, but with slight differences between their ratios (Table 1), and are therefore considered structural isomers with different position of the hydroxyl group on the ring A. Alternatively, TP-14 involves a fragment ion *m/z* 121 instead of 149, suggesting the hydroxylation on ring B (Fig. 1). After MTBSTFA derivatisation, the chromatographic responses of TP-12 and TP-14 decreased by >84%, while the decrease in TP-13 was less significant. Concurrently, a number of new chromatographic peaks appeared in the derivatised samples. At least four of them revealed a MW of 340 $[M]^+$ and, typically, a fragment ion at *m/z*

Table 1. GC-MS retention times, description of EI mass spectra and other relevant data for KP and its TPs

Compound/abbreviation	GC-t_R (min)	*m/z* (% of base peak)	MW	Proposed compound	Generated from	Treatment conditions
Ketoprofen/KP	15.45	254(38), 209(49), 181(22), 177(52), 105(92), 77(100)	254	Parent compound: ketoprofen[a]		
TP-1/EtBP	10.86	210(62), 133(100), 181(32), 105(69), 77(78)	210	3-Ethylbenzophenone[a]	KP	MP
TP-2/AcBP	12.68	224(53), 209(100), 181(17), 147(21), 119(4), 105(88), 77(75)	224	3-Acetylbenzophenone[a]	KP	MP
TP-3	13.18	226(7), 211(36), 183(50), 149(14), 133(34), 105(100), 77(93)	226	3-Acetyl-1,1-diphenylmethanol	KP	MP
TP-4	9.82	196(54), 181(8), 119(100), 105(44), 91(38), 77(30)	196	3-Methylbenzophenone	EtBP	LP
TP-5	9.88	MTBS ester: 266(10), 209(100), 151(4), 149(9), 135(29), 105(3). MS^n: 121	152 (266 MTBS ester)	3-(Hydroxymethyl)-benzoic acid	EtBP	MP
					EtBP	LP
					KP	MP
TP-6	8.49	TMS ester: 236(7), 221(100), 163(0.4), 147(36), 119(8), 105(0.5)	164 (236 TMS ester)	3-Acetyl-benzoic acid	EtBP	LP
					AcBP	LP
TP-7	12.02	TMS ether: 283(12), 270(60), 255(68), 193(7), 181(0.7), 135(18), 105(100)	212 (284 TMS ether)	3-Hydroxymethyl-benzophenone	EtBP	LP
					AcBP	LP + 0.01% H_2O_2
TP-12	11.65	226(80), 225(100), 211(13), 197(9), **149**(31), 133(54), 105(39), 77(84),	226	A-hydroxy-3-ethylbenzophenone	EtBP	LP + 0.01% H_2O_2
TP-13	11.80	226(85), 225(100), 211(8), 197(4), **149**(27), 133(28), 105(38), 77(71)	226		EtBP	LP + 0.01% H_2O_2
TP-14	11.88	226(15), 225(14), 197(100), 133(8), **121**(22), 105(8), 77(9)	226	B-hydroxy-3-ethylbenzophenone	EtBP	LP + 0.01% H_2O_2
TP-12	16.49	MTBS ether: 340(15), 283(100), 105(62), 77(21); MS/MS: 225, 209	226 (340 MTBS ether)	*Isomers*: hydroxy-3-ethylbenzophenone	EtBP	LP + 0.01% H_2O_2
TP-13	17.00	MTBS ether: 340(16), 283(100), 133(37), 105(15), MS/MS: 225, 209			EtBP	LP + 0.01% H_2O_2
TP-14	17.73	MTBS ether: 340(34), 283(99), 105(100), 77(35), MS/MS: 225, 209			EtBP	LP + 0.01% H_2O_2
TP-15	18.24	MTBS ether: 340(38), 283(100), 133(92), 105(30), MS/MS: 225, 209			EtBP	LP + 0.01% H_2O_2
TP-19	13.88	240(82), 225(30), 197(85), **147**(12), **121**(100), 77(12)	240	B-hydroxy-3-acetylbenzophenone	AcBP	LP + 0.01% H_2O_2
TP-20	13.45	240(100), 225(52), **147**(95), 105(7), 77(61)	240	B-hydroxy-3-acetylbenzophenone	AcBP	LP + 0.01% H_2O_2
TP-21	13.65	240(73), 225(60), **163**(100), 105(46), 77(65)	240	A-hydroxy-3-acetylbenzophenone	AcBP	LP + 0.01% H_2O_2
TP-19	14.28	TMS ether: 312(0.2), 297(100)	240(312 TMS ether)	*Isomers*: hydroxy-3-acetylbenzophenone	AcBP	LP + 0.01% H_2O_2
TP-20	15.58	TMS ether: 312(82), 297(100), 269(7)			AcBP	LP + 0.01% H_2O_2
TP-21	16.00	TMS ether: 312(86), 297(100), 223(24), 147(32)			AcBP	LP + 0.01% H_2O_2
TP-22	17.12	TMS ether: 312(58), 297(45), 193(100), 147(53)			AcBP	

[a] Identity of TP confirmed with an authentic standard.

Table 2. LC-MS on the parent compound and the photoproducts formed during UV treatment of ketoprofen[a]

Compound/ abbreviation	LC-t_R (min)	Ionisation mode	Accurate mass (calculated) $[M+H]^+$ or $[M-H]^-$	Mass error (measured)	Elemental composition	MS/MS	MW	Mass difference	Proposed compound	Generated from	Treatment conditions	Cross-confirmed: GC-MS/ (MS)
Ketoprofen/KP	1.2	ESI(+)	$[M+H]^+$ 255.1021	−1.6 ppm	$C_{16}H_{15}O_3$	209, 194, 177, 149, 105, 77	254	0.0000	Parent compound: ketoprofen			+
	3.1	ESI(−)	$[M-H]^-$ 253.0865	−0.8 ppm	$C_{16}H_{13}O_3$	209		0.0000				
TP-1/EtBP	4.2	ESI(+)	$[M+H]^+$ 211.1123	−0.9 ppm	$C_{15}H_{15}O$	158, 141, 133, 105	210	−43.9898	*m*-Ethylbenzophenone[b]	KP	MP	+
TP-2/AcBP	2.9	ESI(+)	$[M+H]^+$ 225.0916	0.0 ppm	$C_{15}H_{13}O_2$	183, 147, 119, 105, 91, 77	224	−30.0105	*m*-Acetylbenzophenone[b]	KP	MP	+
	2.0	ESI(−)	$[M-H]^-$ 223.0759	+0.9 ppm	$C_{15}H_{11}O_2$	181, 119		−30.0106				
TP-8	2.4	ESI(+)	$[M+H]^+$ 227.1072	+1.3 ppm	$C_{15}H_{15}O_2$	209, 194, 183, 149, 121, 105, 77	226	−27.9949	3-(α-Hydroxyethyl)-benzophenone	KP	MP	
										EtBP	LP + 0.01% H_2O_2	
	1.9	ESI(−)	$[M-H]^-$ 225.0916	−2.7 ppm	$C_{15}H_{13}O_2$	210, 182, 120		−27.9949		EtBP	LP	
TP-9	2.7	ESI(+)	$[M+H]^+$ 243.1021	+1.6 ppm	$C_{15}H_{15}O_3$	225, 211, 182, 133, 105	242	−12.0000	3-(1,2-Dihydroxyethyl)-benzophenone	KP	MP	
										EtBP	LP	
TP-10	1.8	ESI(+)	$[M+H]^+$ 243.1021	+1.2 ppm	$C_{15}H_{15}O_3$	225, 210, 199, 121, 105	242	−12.0000	Hydroxy-3-(α-hydroxyethyl)-benzophenone	EtBP	LP	
	1.8	ESI(−)	$[M-H]^-$ 241.0865	+0.0 ppm	$C_{15}H_{13}O_3$	223, 197, 121		−12.0000				
TP-11	1.9	ESI(−)	$[M-H]^-$ 225.0552	+0.4 ppm	$C_{14}H_9O_3$	181	226	−28.0313	3-Benzoyl benzoic acid	AcBP	LP	
										EtBP	LP	
TP-12 to TP-15	3.0	ESI(+)	$[M+H]^+$ 227.1072	−2.6 ppm	$C_{15}H_{15}O_2$	149, 133, 121, 105	226	−27.9949	*Isomers*: hydroxy-3-ethyl-benzophenone	EtBP	LP + 0.01% H_2O_2	+
	3.2	ESI(+)		−1.8 ppm		133, 121				EtBP	LP + 0.01% H_2O_2	+
TP-16	1.6	ESI(+)		+2.6 ppm						EtBP	LP + 0.01% H_2O_2	
TP-17	1.9	ESI(+)		−1.3 ppm						EtBP	LP + 0.01% H_2O_2	
TP-18	2.3	ESI(+)		−1.3 ppm		209, 194, 105			3-(β-hydroxyethyl)-benzophenone	EtBP	LP + 0.01% H_2O_2	
TP-19 and TP-20	2.2	ESI(+)	$[M+H]^+$ 241.0865	+2.1 ppm	$C_{15}H_{13}O_3$	199, **147**, **121**, **119**, 105	240	−14.0156	*Isomers*: B-hydroxy-3-acetylbenzophenone	AcBP	LP + 0.01% H_2O_2	+
	2.3	ESI(+)		−0.4 ppm		199, **147**, **121**, **119**, 105				AcBP	LP + 0.01% H_2O_2	+
TP-21 and TP-22	3.5	ESI(+)		+7.5 ppm		**163**, 147, 145, 121, 105			*Isomers*: A-hydroxy-3-acetylbenzophenone	AcBP	LP + 0.01% H_2O_2	+
	3.7	ESI(+)		+23.6 ppm		**163**, 145, 121, 107, 105				AcBP	LP + 0.01% H_2O_2	+

[a] The fragment ions that define which ring was hydroxylated are in boldcase and underlined.
[b] Identity of TP confirmed by an authentic standard.

Journal of MASS SPECTROMETRY

283 $[M - 57]^+$, corresponding to fragmentation of a *tert*-butyl group from a MTBS derivative. Since the MTBS group is a 115-Da fragment ion, and based on the decrease in the chromatographic response of TP-12 and TP-14 after derivatisation, we assume that these derivatives correspond to MTBS ethers of hydroxylated *m*-EtBP, i.e. TP-12, TP-13, TP-14 and others (TP-15) which were not detected in their underivatised form. In support of this assumption are the results of MS/MS fragmentation obtained by EI ionisation in the IT mass detector. The fragment ion *m/z* 225 is the deprotonated mass of the hydroxylated EtBP and by cleavage of ring hydroxyl group it forms *m/z* 209 (Table 1). Alternatively, in case of a side chain hydroxylation, a loss of a water molecule would have been evident at *m/z* 207. Since all the MTBS derivatives of TP-12–15 show equivalent fragment ions but in different ratios, it is supposed that these compounds are structural isomers differing only in the position of the respective –OH group on the benzophenone ring system. MTBS derivatives have improved GC characteristics compared to their underivatised analogues, which results in higher sensitivity and in turn a higher number of detected compounds. While MTBS derivatives are characterised by a great thermal and hydrolytic stability, the major drawback is the lower reactivity of MTBSTFA compared to other silylating reagents[16] and a slower reaction rate due to steric resistance. Therefore, MTBSTFA was replaced by more a reactive derivatising agent MSTFA in the further experiments.

During photocatalytic irradiation of AcBP, three new compounds (TP-19, TP-20 and TP-21) emerged in GC chromatograms (Table 1). All compounds involve *m/z* 240 in their mass spectra, which is assumed to be their MW. As illustrated in Fig. 1, all three compounds, besides characteristic fragment ions at *m/z* 77 for phenyl and *m/z* 105 for benzoyl, involve also the fragment ion *m/z* 225, which presumably corresponds to a demethylated fragment, analogous to the fragmentation of TP-2 (in this case, the parent compound) at *m/z* 209. TP-19 further shows the fragment ion at *m/z* 197, which corresponds to a hydroxylated benzophenone ring system, similarly as the compounds TP-12, TP-13 and TP-14. In case of TP-19, the fragment ions distinctive for determining, which aromatic ring was hydroxylated were *m/z* 147 and 121 (Table 1, underlined). The first corresponds to 3-acetyl-benzoyl fragment ion and *m/z* 121 analogously with TP-14 indicates a hydroxybenzoyl fragment ion, both of them suggesting that the hydroxylation occurred on the ring B (Fig. 1). Compared to TP-19, TP-20 and TP-21 were more demanding for identification since their area-under-curve only mounted up to 9 and 24% of that of TP-19, respectively. Thus, the mass spectra of TP-20 yielded less fragment ions, but likewise for TP-19, the B-ring hydroxylation is proposed based on the fragment ion at *m/z* 147. Alternatively, TP-21 shows a 16 Da higher *m/z* 163, from which A-ring hydroxylation is assumed. Table 1 shows how after MSTFA derivatisation at least four peaks presumably corresponding to the TMS ethers of hydroxyl-3-AcBP (TP-19–22) appear in the GC chromatogram. All compounds have in common the fragment ion corresponding to the MW of derivative at *m/z* 312 and an abundant fragment ion at *m/z* 297 formed after the cleavage of a methyl group from the TMS ether.

From Table 1, it can be noted that by addition of H_2O_2 to initiate the photocatalytic transformation reactions, the majority of TPs (TP-12–15 formed by photocatalytic transformation of EtBP and TP-19–22 formed from AcBP) was subjected to the hydroxylation of the benzophenone ring system.

Identification by LC-MS

The ESI(+)MS/MS spectrum of protonated KP at $[M + H]^+$ 255 typically gives a decarboxylated fragment ion at *m/z* 209 and 194 after further cleavage of a methyl group. In addition, the ESI(+)MS/MS spectrum shows a phenyl fragment ion (*m/z* 77), a matching 3-(1-carboxyethyl)benzoyl residual at *m/z* 177 to yield the molecular structure as well as a benzoyl fragment ion (*m/z* 105) and a corresponding 3-(1-carboxyethyl)phenyl residual at *m/z* 149. Table 2 further details the mass spectrum of KP acquired under ESI(−) conditions and includes the deprotonated molecule at $[M - H]^-$ 253 and *m/z* 209 formed with the cleavage of CO_2 (Table 2).

The mass spectrum of TP-1 shows a protonated molecule at $[M + H]^+$ 211 and HRMS analysis gives the elemental formula $C_{15}H_{15}O$ at −0.9 ppm mass error. The tandem mass fragmentation of the protonated molecule produced a fragment ion at *m/z* 133 after the cleavage of benzene (*m/z* 77) and, similar to KP, a benzoyl fragment ion at *m/z* 105. According to these data, the TP-1 is proposed to be EtBP which is cross-confirmed by GC-MS. The retention time and the fragmentation of EtBP are also confirmed by comparison with an authentic standard (Table 2).

TP-2 with a protonated molecule at $[M + H]^+$ 225 gives an elemental composition of $C_{15}H_{13}O_2$ and the following fragment ions are evident in the ESI(+) mass spectrum: the *m/z* 147 ($C_9H_7O_2$) for 3-acetylbenzoyl fragment, *m/z* 119 for 3-acetylphenyl, *m/z* 105 for benzoyl, *m/z* 91 for benzyl and the *m/z* 77 for phenyl fragment ion. Furthermore, *m/z* 183 is evident, which corresponds to protonated benzophenone. According to the MS/MS fragmentation and accurate mass determination, the suggested structure of TP-2 is AcBP. The same compound was proposed by GC-MS identification process and was confirmed by comparison to an authentic standard (Table 2).

The accurate mass measurement of the protonated molecule of TP-8 yields the elemental composition $C_{15}H_{15}O_2$, which is two protons higher than AcBP and implies its reduced form. Similar to KP, TP-8 shows fragment ions at *m/z* 209 and 194 corresponding to $C_{15}H_{13}O$ and $C_{14}H_{10}O$, respectively (Table 2). The first fragment ion is formed by the cleavage of H_2O and the second, analogously to KP, after subsequent cleavage of a methyl group. Instead of *m/z* 147 for AcBP, TP-8 shows a hydrogenated residual at *m/z* 149 ($C_9H_9O_2$), i.e. 3-(hydroxyethyl) benzoyl formed by cleavage of a phenyl group from $[M + H]^+$ 227. Analogously to the fragment *m/z* 119 in case of AcBP, TP-8 again produces a hydrogenated form at *m/z* 121 (C_8H_9O). Based on this fragmentation, the TP-8 is identified as 3-(α-hydroxyethyl)-benzophenone.

From Table 2, it is evident that TP-9 has the protonated molecule $[M + H]^+$ 243 with an elemental composition $C_{15}H_{15}O_3$, which suggests the additional oxygenation of the TP-8 molecule. MS/MS fragmentation yields the cleavage of water at *m/z* 225 ($C_{15}H_{13}O_2$) or methanol at *m/z* 211 ($C_{14}H_{11}O_2$) corresponding to a protonated 3-(phenylcarbonyl)-benzaldehyde fragment ion. Therefore, it is supposed that the two oxygen atoms are positioned on the ethyl side chain of the benzophenone ring system (*m/z* 182, $C_{13}H_{10}O$). Further confirmation of the proposed structure is given by the cleavage of a phenyl group at *m/z* 133 ($C_8H_5O_2$). The MS/MS spectrum shows also a typical benzoyl fragment ion at *m/z* 105. The proposed structure of TP-9 is therefore 3-(1,2-dihydroxyethyl)-benzophenone.

TP-10 has the identical elemental composition ($C_{15}H_{15}O_3$) as TP-9 (Table 2), but there are a few decisive fragment ions in its MS/MS spectrum that determine the different position of one hydroxyl group: *m/z* 225 with elemental composition $C_{15}H_{13}O_2$ is

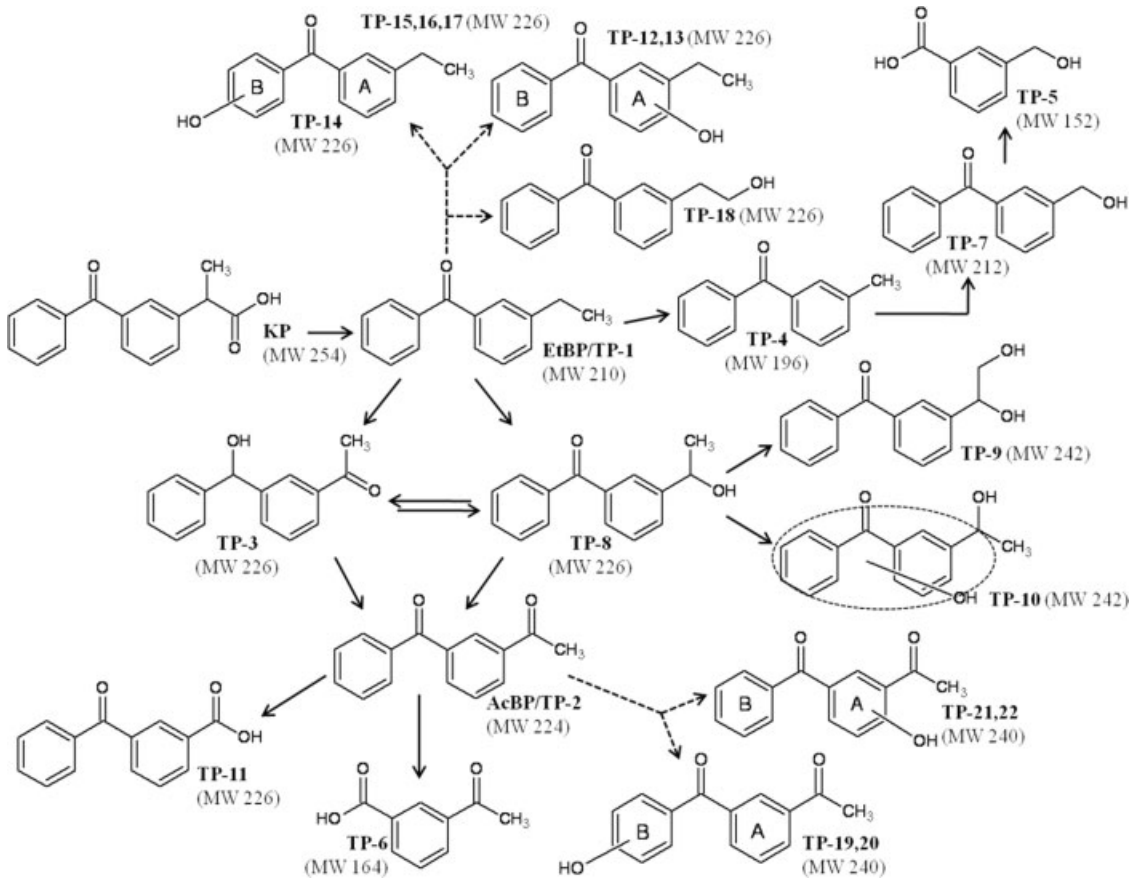

Figure 2. Proposed breakdown pathway.

the result of cleavage of an H_2O molecule, and *m/z* 210 ($C_{14}H_{10}O_2$) if formed by the subsequent cleavage of a methyl group. This implies that one –OH group is positioned on the side chain, presumably at α-position, where oxidation typically takes place. In contrast to TP-9, the mass spectrum of this compound involves *m/z* 199 ($C_{13}H_{11}O_2$) representing a hydroxylated benzophenone, and *m/z* 121 ($C_7H_5O_2$), a hydroxy-benzoyl fragment. In regards to the latter two fragment ions, it is assumed that the second hydroxyl group is positioned on the benzophenone ring system and TP-10 is identified as hydroxy-3-(α-hydroxyethyl)-benzophenone.

As evident from Table 2, TP-11 was found after LP-UV treatment of AcBP samples and was detected only in ESI(−) mode, showing a deprotonated molecule at $[M - H]^-$ 225. The accurate mass measurement gave an elemental composition of $C_{14}H_9O_3$. The ESI(−)MS/MS fragmentation resulted in the formation of *m/z* 181 ($C_{13}H_9O$), suggesting a deprotonated benzophenone, analogously to the parent compound AcBP. The latter is formed by the cleavage of CO_2, which is a typical dissociation of a carboxylic acid in ESI(−) mode. According to these data, the assigned structure of TP-11 is 3-benzoylbenzoic acid.

During photocatalytic degradation of EtBP with 0.01% H_2O_2 at least six new peaks are revealed in the LC-MS chromatogram (TP-8 and TP-12–18; Table 2). All TPs show a protonated molecule at $[M + H]^+$ 227, and accurate mass measurements reveal their common elemental composition $C_{15}H_{15}O_2$. This implies that these TPs are isomeric oxygenated EtBP derivatives. TP-16 and TP-17 (Table 2) eluted at 1.6 and 1.9 min, respectively, and were unfortunately not sufficiently abundant to enable their structural elucidation by CID. Furthermore, considering the retention time and MS/MS spectra, the TP eluting at 2.4 min is assigned as TP-8 [3-(α-hydroxyethyl)-benzophenone], which has been previously identified as a product of photolytic breakdown of KP and EtBP (Table 2). As illustrated in Table 2, TP-18 elutes 0.1 min prior to TP-8 and shows an MS/MS spectrum strongly related to that of TP-8. According to its fragment ion *m/z* 209 ($C_{15}H_{13}O$), which is indicative for the cleavage of water from $[M + H]^+$ 227, TP-18 involves a hydroxyl group on the side chain and, being a structural isomer of TP-8, the only feasible position of the hydroxyl group is on β-carbon of the ethyl group. For these reasons, the chemical structure of TP-18 is assigned as 3-(β-hydroxyethyl)-benzophenone. The remaining two TPs formed by photocatalytic breakdown of EtBP elute at 3.0 and 3.2 min, and show similar ESI(+)MS/MS patterns (Table 2), which are further related to those produced by EI of TP-12–15 (Fig. 1). It is therefore assumed that the compounds detected at 3.0 and 3.2 min in the LC chromatograms are representatives of ring-hydroxylated benzophenones, assigned in Tables 1 and 2 as TP-12–15.

By exposing AcBP to photocatalysis, four peaks are revealed in the LC chromatograms, where two, TP-19 and TP-20, and two, TP-21 and TP-22, elute close together (Table 2). All four TPs show the same protonated molecule $[M + H]^+$ 241 and the elemental composition $C_{15}H_{15}O_3$; though, the accurate mass determination gives an unusually high mass error (+7.5 and +23.6 ppm, Table 2) in case of TP-21 and TP-22, which may be the consequence of their low abundance. Table 2 illustrates most notable ESI(+)MS/MS fragment ions, where the decisive ones are underlined. The mass spectra of TP-19 and TP-20, analogously to TP-10, involve *m/z* 199 ($C_{13}H_{11}O_2$) representing a hydroxylated benzophenone.

Journal of MASS SPECTROMETRY

Furthermore, *m/z* 147 ($C_9H_7O_2$) and *m/z* 119 (C_8H_7O) both match the parent compound AcBP and stand for 3-acetylbenzoyl and acetylphenyl fragment ion, respectively. Furthermore, *m/z* 121 ($C_7H_5O_2$) is a hydroxy-benzoyl fragment and again implies a hydroxylation. From these data, it is assumed that TP-19 and TP-20 represent isomeric B-ring hydroxylated-3-AcBPs, which is cross-confirmed by EI ionisation as observed in Table 1 and Fig. 1. In contrast to TP-19 and TP-20, the mass spectra of TP-21 and TP-22 yield *m/z* 163 ($C_9H_7O_3$), which is 16 Da or one oxygen higher than *m/z* 147 ($C_9H_7O_2$), suggesting that the hydroxylation in this case occurs on the A-ring of the benzophenone ring system. Again this assumption is confirmed by EI fragmentation, as evident in Table 1 and Fig. 1.

Linking the polarity of KP and its TPs with their elution order we observe that in LC, the parent compound elutes first (1.2 min). Given the pK_a of 4.7 for this weak acid,[14] the negatively charged species is the dominant form under given LC conditions, thus yielding low interactions with the LC column. On the contrary, EtBP is not charged, and gives less polar interactions with the mobile phase than other TPs, therefore it elutes at 4.1 min (Table 2). The elution order is generally reverse in case of the GC separation, where the least polar compounds *m*-methylbenzophenone and *m*-ethylbenzophenone reach the mass detector before the more polar hydroxylated TPs (Table 2).

Identity confirmation with authentic standards

To enable further insight into the photodegradation pathway of KP, and to confirm the identities of the proposed TPs, the two compounds EtBP and iPrBP, initially proposed on the basis of their GC-MS fragmentation, were synthesised. An authentic standard of the third proposed compound (AcBP) was purchased. To confirm the identity of the proposed TPs with reference standards, we referred to the following acceptability criteria[19]: Ion ratios for a given TP, measured as the peak area of a quantitation ion divided by the peak area of the qualifier ion should be within ±20% of the average of the reference compounds' ion ratios, and the TP was required to have a retention time within ±0.20 min of the reference compounds' average retention time. From Table 3, it is evident that EtBP and AcBP clearly meet these requirements, whereas iPrBP failed to be identified as the TP.

Furthermore, Table 3 shows how both iPrBP and AcBP share the same principal fragment ions, and also their mass spectra are similar (data not shown). It was therefore not possible to distinguish between the two compounds based only on their EI fragmentation pattern, and the comparison with the reference compound was in this case crucial to confirm the identity of AcBP. As follows, EtBP and AcBP were individually tested on their breakdown and further fate under UV irradiation, whereas iPrBP was excluded from further research.

The breakdown pathway

The proposition of a UV breakdown scheme of KP was based on the treatment experiments with three individual reference standards, i.e. KP, EtBP and AcBP. In respect to the formation of both EtBP and AcBP in treated KP samples, the formation of solely AcBP in treated EtBP samples, and the absence of both EtBP and KP in the treated AcBP samples, we assume that the fundamental breakdown pathway follows as KP → EtBP → AcBP (Fig. 2). In agreement with the literature,[20–22] which reported KP to be one of the most rapidly degrading pharmaceuticals, we achieved very fast transformation of KP. Conversely, KP transformation products EtBP and AcBP were found more resistant to both MP and LP irradiation. It is therefore assumed that in the aqueous environment, KP easily transforms into its major product EtBF and into AcBP, which would persist longer.

TP-3 and TP-8 are hydrogenated analogues of AcBP with a tautomeric position of the –OH group, which were absent in the treated AcBP samples, whereas they occurred in treated EtBP samples. Therefore, TP-3 and TP-8 are considered intermediates in the oxidative formation of AcBP from EtBP. As evident from Fig. 2, TP-9 and TP-10 are formed by subsequent hydroxylation of TP-8 on the α-hydroxyethyl side chain and benzophenone ring system, respectively.

Figure 2 illustrates an alternative UV-breakdown pathway of EtBP implying a side chain shortening (TP-4) and side chain hydroxylation (TP-7), followed by an oxidative cleavage of the benzophenone ring system (TP-5). A structurally related *m*-substituted benzoic acid is TP-6, which is formed by the oxidative cleavage of benzophenone ring system from AcBP. Alternatively, an oxidative transformation on the acetyl side chain of AcBP leads to the formation of 3-benzoylbenzoic acid (TP-11). TP-5 and TP-6 are important UV-breakdown products, since they cease further formation of phototoxic benzophenone TPs, whereas all the remaining compounds still involve the benzophenone moiety (Fig. 2). Ironically, in spite of their photo-induced adverse effects, certain benzophenone derivatives are still used as sunscreens,[23] due to their recognised ability to absorb UVA and UVB light.

Whereas OH radicals are hardly involved in degradation of KP,[24] Fig. 2 distinguishes TP-12–18 and TP-19–22 from other

Table 3. Confirmation of EtBP and AcBP by authentic standards based on their retention time, NIST 98 similarity and quantifier and qualifier ions' ratio

Compound		EtBP	iPrBP	AcBP
Retention time (min)	Reference	10.91	11.37	12.68
	Analyte	10.86	12.68	12.68
NIST 98 probability (%)	Reference	93	95	No relevant hits
	Analyte	93	No relevant hits	No relevant hits
Quantifier/qualifier 1	Reference	*m/z* 133/210 = 1.5	*m/z* 209/224 = 0.86	*m/z* 209/224 = 2.0
	Analyte	*m/z* 133/210 = 1.6	*m/z* 209/224 = 2.0	*m/z* 209/224 = 2.0
Quantifier/qualifier 2	Reference	*m/z* 133/181 = 2.8	*m/z* 209/181 = 2.7	*m/z* 209/181 = 6.1
	Analyte	*m/z* 133/181 = 3.0	*m/z* 209/181 = 6.4	*m/z* 209/181 = 6.4
Outcome		Confirmed	Failed	Confirmed

compounds by a dashed arrow and classifies them into a group of compounds formed strictly by a photocatalytic transformation of EtBP or AcBP, respectively. Except for TP-18, which was subjected to a side-chain hydroxylation, the remaining six photocatalytic TPs of EtBP (TP-12 to TP-17) involve a hydroxyl group positioned on the benzophenone ring system. Similarly, the photocatalytic TPs of AcBP were hydroxylated either on the A-ring (TP-21 and TP-22) or on the B-ring (TP-19 and TP-20) of the benzophenone ring system. This finding is in agreement with Hayashi *et al*.,[25] who suggests an enhanced hydroxylation of benzophenone ring system in the presence of H_2O_2. Such transformations may not only occur during water treatment but also in the environment, where photosensitisers such as humic acids generate reactive oxygen species causing the ring hydroxylation of benzophenone derivatives. Benzophenone is a suspected endocrine-disrupting chemical.[25] Whereas the estrogenic activity was not shown for the compound itself, it was found that benzophenone acquired estrogenic activity after ring hydroxylation.[25] As evident in Fig. 2, the ring hydroxylation occurred in 11 of 22 identified TPs, and there exists a strong indication that these compounds are endocrine disruptors, which calls for further estrogenic activity testing.

Nevertheless, it should be stressed that the proposed UV breakdown scheme is configured based on treatment experiments using only three reference standards. Therefore, the proposed breakdown scheme cannot be regarded as complete and warrants confirmation by reference standards of the remaining TPs.

CONCLUSIONS

This study highlights the transformation of the widely used pharmaceutical KP under exposure to UV irradiation. Using complementary chromatographic and mass spectrometric techniques, i.e. gas chromatography coupled to single quadrupole or ion trap mass spectrometry and liquid chromatography hyphenated with QqToF mass spectrometry, we were able to propose chemical structures of 22 TPs of KP, 18 of which are novel. The identified compounds were used to construct a breakdown pathway showing that, in given experimental conditions, neither UV nor the photocatalytic treatment led to a complete mineralisation of the parent compound KP. Instead, 20 of the TPs retained the benzophenone moiety, which causes photo-allergic reactions. Additionally, since benzophenone derivatives may also be formed in the aqueous environment or during water treatment, such symptoms can be generated after contact with environmental or tap water containing such compounds. Another risk arises from hydroxylated benzophenones formed during the photocatalytic transformation of KP, since they show a potential estrogenic effect. Hopefully, this study will increase attention into the transformation of pharmaceuticals and possible risks related to their presence in the environment, which should encourage further research into more efficient treatment technologies to limit the entrance of such compounds into the environmental or drinking waters.

Acknowledgements

The authors kindly acknowledge the financial support given by the Slovenian Research Agency (Program group P1-0143). For their support and helpful advice the authors are grateful to Ms Silvia Pirš (Jožef Stefan Institute, Slovenia), Dr Oliver Bajt (National Institute of Biology, Marine Biological Station, Slovenia), Dr David Heath (Jožef Stefan International Postgraduate School, Ljubljana, Slovenia), Prof. Jurij Svete and Rok Prebil (Faculty of Chemistry and Chemical Technology, University of Ljubljana, Slovenia).

REFERENCES

[1] R. F. Borne. In *Principles of Medicinal Chemistry*, 4th ed., T. L. Lemke, D. A. Williams, W. O. Foye (Eds). Williams & Wilkins: PA, USA, **1995**, 535.
[2] European Medicines Agency, Committee for Medicinal Products for Human Use (CHMP), *Press release: European Medicines Agency confirms positive benefit-risk balance of topical formulations of ketoprofen*. European Medicines Agency: **2010**, EMA/CHMP/465633/2010.
[3] S. Ophaswongse, H. Maibach. Topical nonsteroidal antiinflammatory drugs: allergic and photoallergic contact dermatitis and phototoxicity. *Contact Dermatitis.* **1993**, *29*, 57.
[4] M. C. Marguery, N. Chouini-Lalanne, J. C. Ader, N. Paillous. Comparison of the DNA damage photoinduced by fenofibrate and ketoprofen, two phototoxic drugs of parent structure. *Photochem. Photobiol.* **1998**, *68*, 679.
[5] T. Kosjek, E. Heath, A. Krbavčič. Determination of non-steroidal anti-inflammatory drug (NSAIDs) residues in water samples. *Environ. Int.* **2005**, *31*, 679.
[6] N. M. Vieno, T. Tuhkanen, L. Kronberg. Seasonal variation in the occurrence of pharmaceuticals in effluents from a sewage treatment plant and in the recipient water. *Environ. Sci. Technol.* **2005**, *39*, 8220.
[7] A. Lahoz, D. Hernandez, M. A. Miranda, J. Perez-Prieto, I. M. Morera, J. V. Castell. Antibodies directed to drug epitopes to investigate the structure of drug-protein photoadducts. Recognition of a common photobound substructure in tiaprofenic acid/ketoprofen cross-photoreactivity. *Chem. Res. Toxicol.* **2001**, *14*, 1486.
[8] A. Radschuweit, H.-H. Ruttinger, P. Nuhn, W. Wohlrab, Chr. Huschka. UV-induces formation of hydrogen peroxide based on the photochemisty of ketoprofen. *Photochem. Photobiol.* **2001**, *73*, 119.
[9] F. Bosca, M. A. Miranda. Photosensitizing drugs containing benzophenone chromophore. *J. Photochem. Photobiol. B*, **1998**, *43*, 1.
[10] F. Boscá, M. A. Miranda, G. Carganico, D. Mauleon. Photochemical and photobiological properties of ketoprofen associated with the benzophenone chromophore. *Photochem. Photobiol.* **1994**, *60*, 96.
[11] A. Nakajima, M. Tahara, Y. Yoshimura, H. Nakazawa. Determination of free radicals generated from light exposed ketoprofen. *J. Photochem. Photobiol. A*, **2005**, *174*, 89.
[12] F. Bosca, M. L. Marın, M. A. Miranda. Photoreactivity of the non-steroidal anti-inflammatory 2-arylpropionic acids with photosensitizing side effects. *Photochem. Photobiol.* **2001**, *74*, 637.
[13] F. Bosca, G. Carganicob, J. V. Castell, M. J. Gomez-Lechon, D. Hernandez, D. Mauleon, L. A. Martinez, M. A. Miranda. Evaluation of ketoprofen (R, S and R/S) phototoxicity by a battery of in vitro assays. *J. Photochem. Photobiol. B*, **1995**, *31*, 133.
[14] K. A. K. Musa, J. M. Matxain, L. A. Eriksson. Mechanism of photo-induced decomposition of ketoprofen. *J. Med. Chem.* **2007**, *50*, 1735.
[15] C. Prakash, C. L. Shaffer, A. Nedderman. *Mass Spectrom. Rev.* **2007**, *26*, 340.
[16] T. Kosjek. *Occurrence, fate and removal of pharmaceutical residues in water treatment*. *Doctoral dissertation.* Ljubljana Jožef Stefan International Postgraduate School, **2009**.
[17] K. L. Woo, J. I. Kim. New hydrolysis method for extremely small amount of lipids and capillary gas chromatographic analysis as N(O)-tert.-butyldimethylsilyl fatty acid derivatives compared with methyl ester derivatives. *J. Chromatogr. A*, **1999**, *862*, 199.
[18] M. Farré, M. Petrović, D. Barceló. Recently developed GC/MS and LC/MS methods for determining NSAIDs in water samples. *Anal. Bioanal. Chem.* **2007**, *387*, 1203.
[19] B. W. Brooks, C. K. Chambliss, J. K. Stanley, A. Ramirez. Determination of select antidepressants in fish from an effluent dominated stream. *Environ. Toxicol. Chem.* **2005**, *24*, 464.
[20] I. Kim, N. Yamashita, H. Tanaka. Performance of UV and UV/H2O2 processes for the removal of pharmaceuticals detected in secondary effluent of a sewage treatment plant in Japan. *J. Hazard. Mater.* **2009**, *166*, 1134.

[21] V. J. Pereira, K. G. Lindenb, H. S. Weinberg. Evaluation of UV irradiation for photolytic and oxidative degradation of pharmaceutical compounds in water. *Water Res.* **2007**, *41*, 4413.
[22] I. Kim, H. Tanaka. Photodegradation characteristics of PPCPs in water with UV treatment. *Environ. Int.* **2009**, *35*, 793.
[23] A. C. de Groot, J. P. Nater, J. W. Weyland. *Unwanted Effects of Cosmetics and Drugs Used in Dermatology*, 3rd ed. Elsevier Science B.V.: Amsterdam, **1994**.
[24] I. Kim, N. Yamashita, H. Tanaka. Photodegradation of pharmaceuticals and personal care products during UV and UV/H2O2 treatments. *Chemosphere* **2009**, *77*, 518.
[25] T. Hayashi, Y. Okamoto, K. Ueda, N. Kojima. Formation of estrogenic products from benzophenone after exposure to sunlight. *Toxicol. Lett.* **2006**, *167*, 1.

